Supplementary Information

For

Molecular Control over Vitrimer-like Mechanics – Tuneable Dynamic Motifs based on the Hammett Equation in Polyimine Materials

Sybren K. Schoustra,[a] Joshua A. Dijksman,[b] Han Zuilhof,[a,c,d] Maarten M. J. Smulders*,[a]

[a] Laboratory of Organic Chemistry, Wageningen University, Stippeneng 4, 6708 WE Wageningen, The Netherlands. [b] Physical Chemistry and Soft Matter, Wageningen University, Stippeneng 4, 6708 WE Wageningen, The Netherlands. [c] School of Pharmaceutical Sciences and Technology, Tianjin University, 92 Weijin Road, Tianjin, China. [d] Department of Chemical and Materials Engineering, Faculty of Engineering, King Abdulaziz University, Jeddah, Saudi Arabia.

* Corresponding author: maarten.smulders@wur.nl

Table of content

1. Materials and Methods

All solvents (tetrahydrofuran, dichloromethane, methanol, heptane, acetonitrile, $CDCl_3$, acetone-d_6) were bought from either Sigma-Aldrich, Tokyo Chemical Industry (TCI) or Alfa Aeser and used as received (unless indicated differently). Terephthalaldehyde (**TA**, 99%), 4,4'-diaminobenzophenone (**KDA**, 97%), and 4,7,10-trioxa-1,13-tridecanediamine (**TOTDDA**, 97%) were bought from Sigma-Aldrich. 4,4'-diaminophenyl sulfone (**SDA**, 97%), 4,4'-(hexafluoroisopropylidene)dianiline (**FDA**, 98%) and tris(2-aminoethyl)amine (**TREN**, 97%) were bought from Acros Organics. 4,4-Thiodianiline (**TDA**, 98%) and 4,4'-oxydianiline (**ODA**, 98%) were bought from Tokyo Chemical Industry (TCI).

NMR spectra were recorded on a Bruker Avance III 400 MHz instrument and analysed with MestreNova software. Chemical shifts are reported in parts per million (ppm), calibrated on the residual peak of the solvent, whose values are referred to tetramethylsilane (TMS, δ_{TMS} = 0 ppm), as the internal standard. IR analyses were performed on a Bruker Tensor 27 spectrometer with platinum ATR accessory. Rheological measurements were conducted on an MCR 301 Anton Paar rheometer in combination with a temperature-controlled plate-plate configuration and temperature controller hood for additional thermal homogeneity. Dynamic mechanical analysis (DMA) was performed on a Q800 TA Instruments machine with film tension clamp.

1.1 Small-molecule exchange studies: equilibrium studies

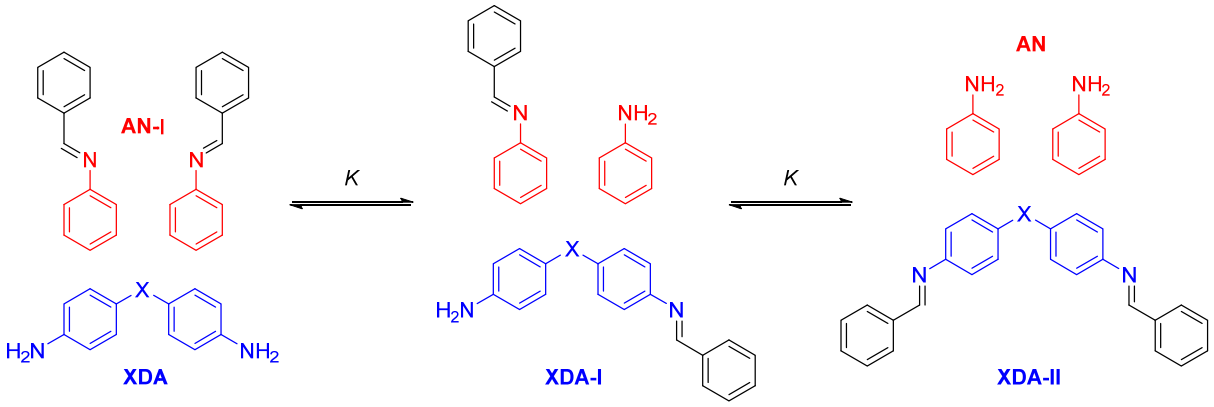

*Scheme S1 Exchange reaction of aromatic imine with tuneable dianiline monomers. For the equilibrium constant (K) experiment 0.5 equivalents of **XDA**, with respect to **AN-I** was added to obtain a 1:1 imine:amine ratio. For the reaction rate (k) experiment 5 equivalents of **XDA** were added to obtain a 1:10 imine:amine ratio.*

Benzaldehyde (0.04 mmol, 4.1 µL) and aniline (0.04 mmol, 3.7 µL) were dissolved in $CDCl_3$ to form the reference imine (**AN-I**). Then the tuneable dianiline (**XDA**) (0.02 mmol, corresponding to approx. 4 mg, depending on the dianiline) was added. The mixture was left at room temperature for several days until exchange equilibrium was reached, as concluded from ^{1}H NMR. Once equilibrium had reached, the ratio of formed imines was determined via integration of the appropriate NMR signals. In most cases this was done by integrating the imine peaks, unless these overlapped. When an overlapping imine signal was present, integration of a different (non-overlapping) signal was performed. The following equation was used to derive the overall equilibrium constant (*K*):

$$K = \frac{[aniline\ amine][XDA\ imine]}{[XDA\ amine][aniline\ imine]} \qquad \text{(Equation S1)}$$

Note that both amine groups of the dianiline each count for one reactive species. Therefore, the initial amine groups of the aniline and dianiline are equivalent. Thus, we can also state that [aniline amine] = [**XDA** imine] and [**XDA** amine] = [aniline imine]. The equation then becomes:

$$K = \frac{[XDA\ imine]^2}{[aniline\ imine]^2} = \left(\frac{[XDA\ imine]}{[aniline\ imine]}\right)^2 \qquad \text{(Equation S2)}$$

The concentration of both imines can be determined from simple integration of their corresponding ^{1}H NMR signal integrals. Log(*K*) could then be plotted for all dianilines as function of *σ* to obtain a Hammett plot (see Fig. 1, main article), assuming that *K* is the same for both reaction steps (Scheme S1). All determined *K* values are also presented in Table S1.

Table S1 Overview of determined equilibrium constants (K) and reaction rate constants (k). For the reaction rate experiment, the solvent was changed from $CDCl_3$ to acetone-d_6 as a consequence of poorer solubility of the dianilines due to the higher required concentration. For the same reason, ***ODA*** *was excluded from this experiment.*

XDA	*K*	*k* [min^{-1}]
ODA	3.92 ± 0.05	–
TDA	$3.14 \pm 0.04 \cdot 10^{-1}$	$6.61 \pm 0.15 \cdot 10^{-2}$
KDA	$5.75 \pm 0.13 \cdot 10^{-2}$	$2.63 \pm 0.12 \cdot 10^{-2}$
FDA	$1.23 \pm 0.03 \cdot 10^{-2}$	$1.26 \pm 0.09 \cdot 10^{-3}$
SDA	$1.20 \pm 0.03 \cdot 10^{-2}$	$1.12 \pm 0.10 \cdot 10^{-4}$

1.2 Small-molecule exchange studies: kinetic studies

N-benzylideneaniline (1.81 mg, 0.01 mmol) was dissolved in 0.6 mL of acetone-d_6. Then, the tuneable dianiline (0.05 mmol, approximately 10 mg, depending on the nature of the dianiline) was added to the mixture. ^{1}H NMR was used to check the conversion of the exchange reaction over time by simple integration (Fig. S1–S4, signals used for integration are highlighted). The conversion into the product was plotted as a function of the time, and curves were fitted according to a first-order reaction rate law:

$$y = A * (1 - e^{-k*t}) \qquad \text{(Equation S3)}$$

The reaction rate constant (*k*) was derived from the fitted curves (Fig. S5), and subsequently, the obtained *k* values were plotted as a function of the Hammett parameter (*σ*) of the tuneable dianilines (see Fig. 1, main article). All determined *k* values are also presented in Table S1. To allow for the possibility for an incomplete conversion (which is inherently possible for a dynamic covalent bond formation reaction), the value of *A* was

included as a fit parameter to find the value to which the conversion converged (*i.e.*, the maximum value for *A* was 100).

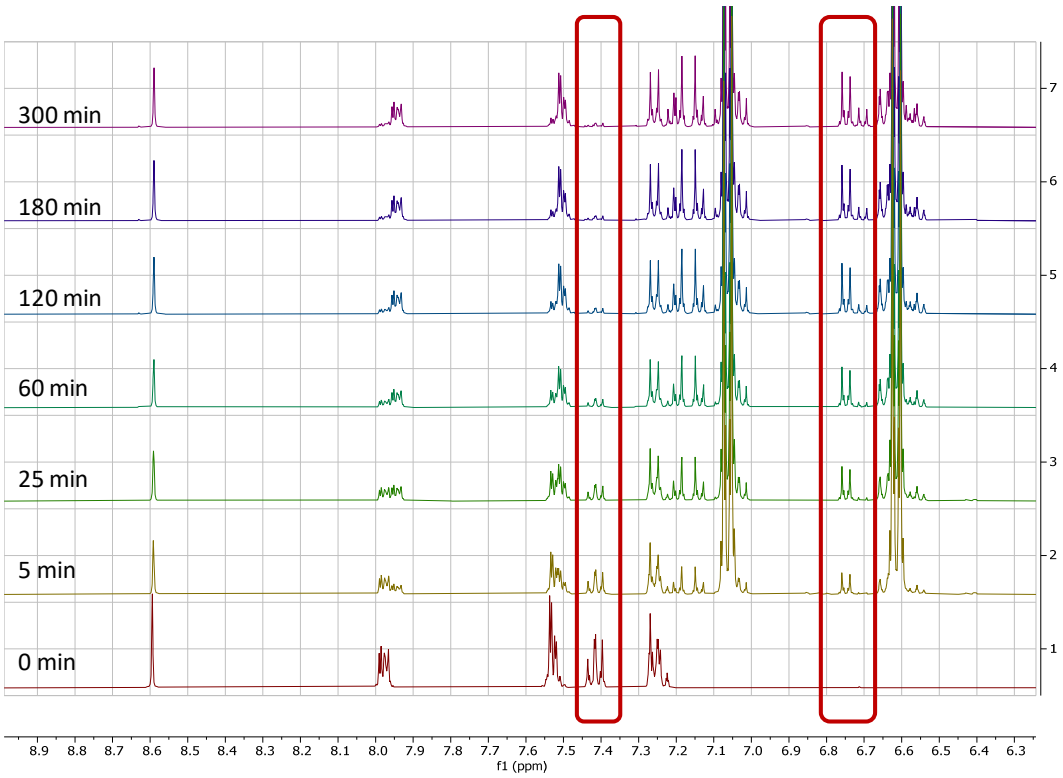

*Fig. S1 ^{1}H spectra at indicated time points for the imine exchange reaction with **TDA**. The signals of the starting imine material (highlighted peak at 7.41 ppm) decreases over time, whereas the signal for the **TDA** imine (highlighted at 6.75 ppm for mono substituted and 6.70 ppm for disubstituted) increases.*

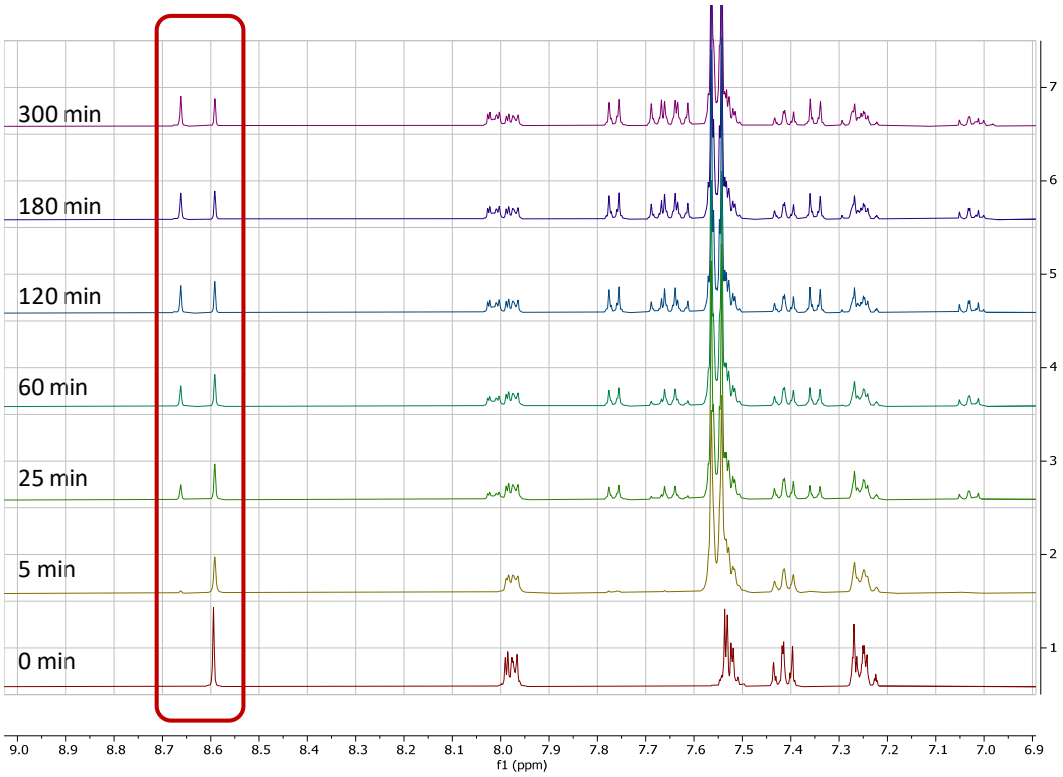

*Fig. S2 ^{1}H spectra at indicated time points for the imine exchange reaction with **KDA**. The signals of the starting imine material (highlighted peak at 8.59 ppm) decreases over time, whereas the signal for the **KDA** imine (highlighted at 8.66 ppm) increased.*

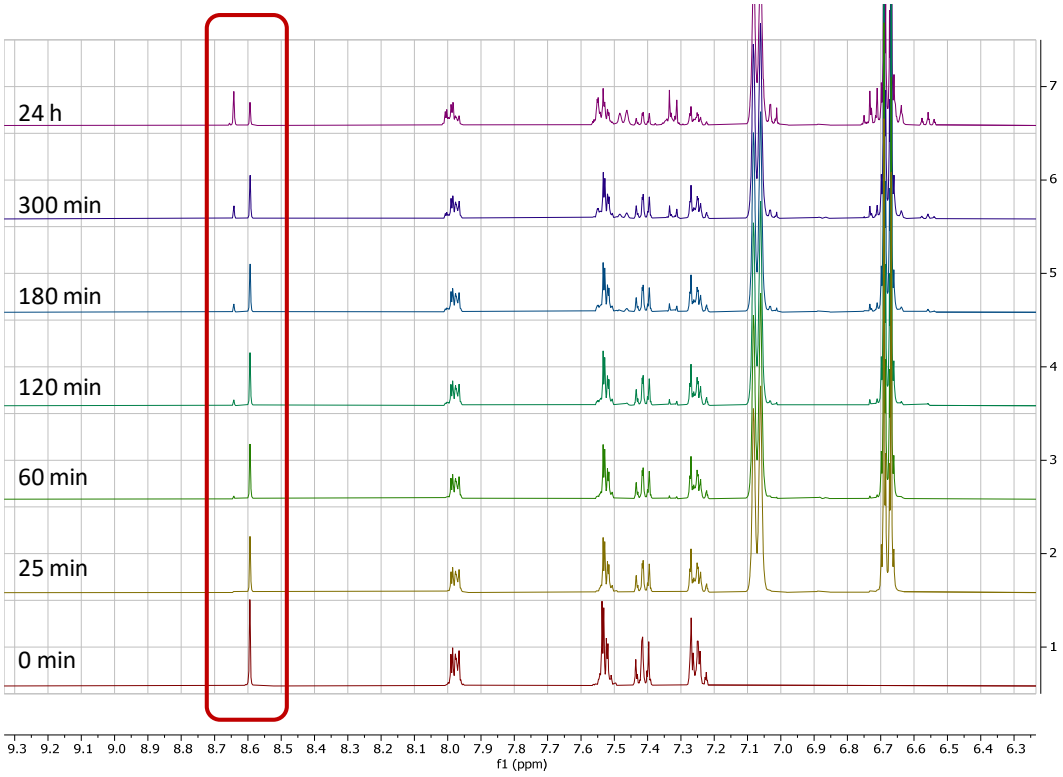

*Fig. S3 ^{1}H spectra at indicated time points for the imine exchange reaction with **FDA**. The signals of the starting imine material (highlighted peak at 8.59 ppm) decreases over time, whereas the signal for the **FDA** imine (highlighted at 8.64 ppm) increased.*

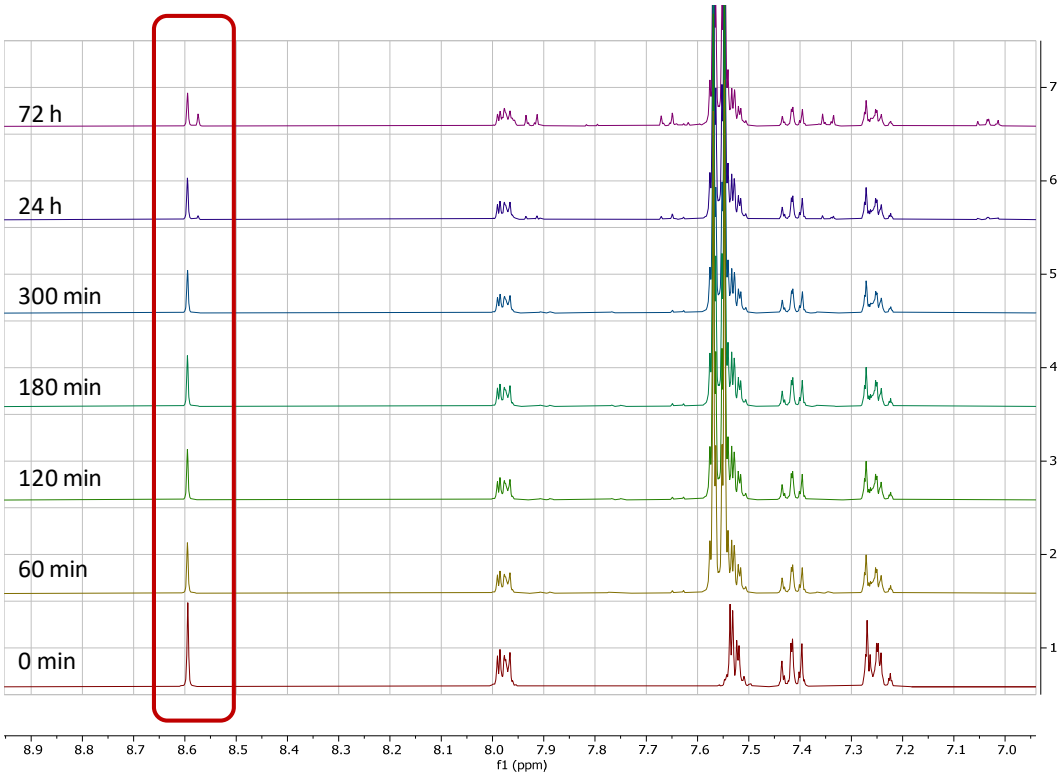

*Fig. S4 [1]H spectra at indicated time points for the imine exchange reaction with **SDA**. The signals of the starting imine material (highlighted peak at 8.59 ppm) decreases over time, whereas the signal for the **SDA** imine (highlighted at 8.57 ppm) increased.*

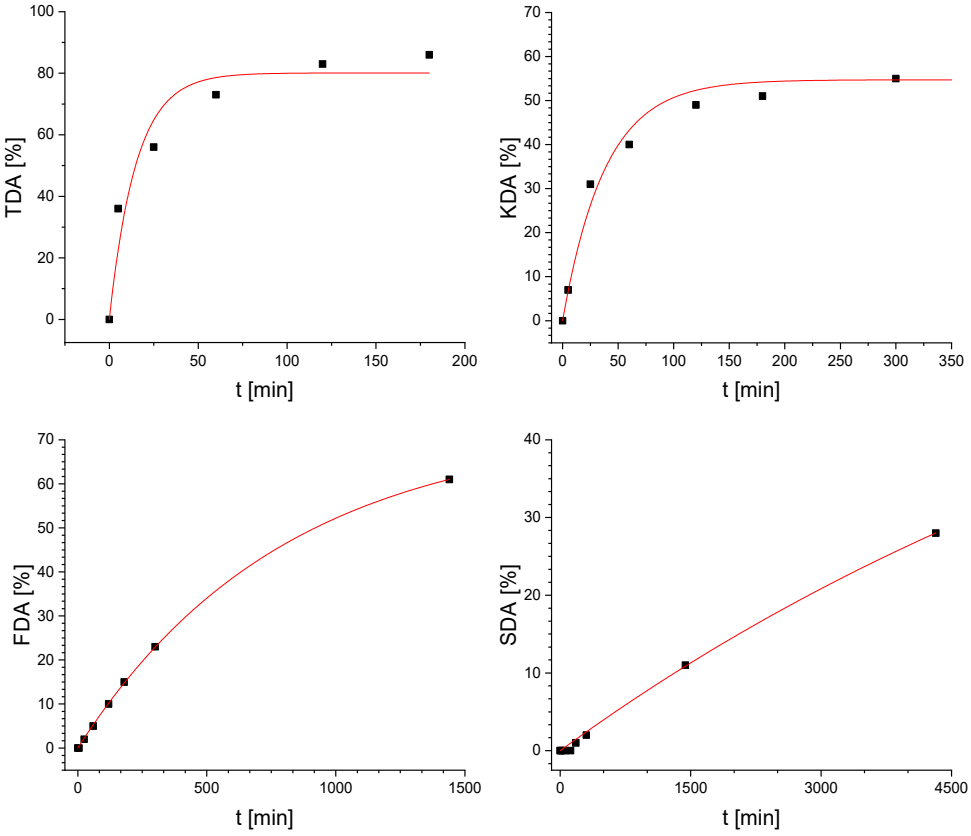

Fig. S5 Overview of the kinetic data and best-fitted curves for estimation of the reaction rate constants. The results of the fitting have been included in Table S1.

1.3 General synthesis of polyimine networks

The tuneable dianiline (0.80 mmol, corresponding to approx. 180 mg, depending on the nature of the tuneable dianiline), **TREN** (0.20 mmol, 30 µL) and **TOTDDA** (2.90 mmol, 0.64 mL) were mixed together in THF (5.0 mL). Terephthalaldehyde (4.00 mmol, 537 mg) was then added to the mixture at room temperature, and the mixture was briefly shaken until a homogeneous solution was obtained. The solution was poured into a petri dish and was left for overnight to slowly evaporate the solvent. The samples were further dried in a vacuum oven at 50 °C for 3 more nights. Afterwards, the materials were cooled to room temperature and FT-IR spectroscopy was used to check the conversion from aldehyde (signal ~1700 cm^{-1}) to imine (~1640 cm^{-1}).

1.4 Rheology experiments

Discs with a 10 mm diameter and a 0.4 mm thickness were prepared by hot-pressing the synthesised **P-XDA** polymer materials at a maximum temperature of 75 °C and maximal force of 40 N.

Four types of rheology experiments were performed: stress relaxation, a creep experiment, frequency sweeps at several temperatures, and a temperature sweep.

In the *stress relaxation* tests, the discs were subjected to a constant strain of 1% and the relaxation modulus (G) was followed over time. The experiment was carried out for all materials at temperatures from 10–50 °C, with increments of 5 °C. After every measurement, the stress was brought back to 0 and the samples were given 10 minutes to reach the new temperature. The normalised relaxation modulus (G/G_0) was plotted against the time to obtain the relaxation curves. The relaxation time (τ), where $G/G_0 = 1/e$ according to the Maxwell model for stress relaxation ($G/G_0 = \exp[-t/\tau]$), was then interpolated for every temperature curve to construct an Arrhenius plot. This plot was derived by plotting $\ln(\tau)$ against the reciprocal temperature ($1/T$). The kinetic activation energy (E_a) was calculated from the slope of the fitted line multiplied by the gas constant

(R = 8.3145 J K^{-1} mol^{-1}). The E_a values were derived for all materials and were then plotted as a function of their corresponding Hammett value (σ).

The *creep* test was performed by exposing each polymer disc to a constant stress of 10 kPa and following the strain (γ) over time, which was subsequently plotted for every material. The temperature was held constant at 20 °C. A constant point in time of 100 s was taken to derive the total amount of strain in the given time frame. The total strain at 100 s was then plotted against the Hammett parameter (σ) of the corresponding material.

Frequency sweeps were carried out on the polymer discs at angular frequency (ω) range of 0.1–100 Hz, and an applied strain of 0.1%. The measurement was performed at 25, 50, 75 and 100 °C. The storage (G') and loss (G'') modulus were consequently plotted as a function of the frequency at all given temperatures for all **P-XDA** materials.

Temperature sweeps were performed on the polymer discs on temperature range from 0–150 °C with a constant angular frequency of 1 Hz and strain of 0.1%. Storage (G') and loss (G'') moduli were measured as a function of the temperature. Tan(δ) was calculated as G''/G' and was also plotted as a function of the temperature. The materials with the most electron-donating substituents (**P-ODA** and **P-TDA**) displayed a peak in tan(δ), and therefore T_g was determined from the top of this peak.[S1] For the materials with more electron-withdrawing groups (**P-KDA**, **P-FDA** and **P-SDA**), a point in temperature was reached at which the G' rapidly drops to 0. For these materials T_g was determined at the point where tan(δ) = 1.[S2] The rubbery domain of the materials was taken as the temperature range over which a constant plateau value was observed in the G' curve.

1.5 Thermal stability test

Thermal stability was tested using thermographic analysis (TGA). Small pieces (10 mg) of the **P-XDA** materials were loaded and heated on a temperature ramp of 30–900 °C with a heating speed of 1 °C per minute. The total remaining weight percentage was followed as a function of the temperature.

1.6 Solubility experiment

A small piece of the **P-XDA** material (20 mg) was cut off and placed in a vial containing 2 mL of a specific solvent (water, THF, acetonitrile, DCM, methanol or heptane). The vials were capped and left for 5 days at room temperature. The non-dissolved solid was removed from the vial and dried to air for overnight, followed by drying *in vacuo* at 50 °C for another day. The dried solids were weighed and the non-soluble fraction was determined as the weight after the experiment divided by the weight of the initial sample. For the NMR experiment, approx. 4 mg of **P-ODA** was added to an NMR tube and then dissolved in the specified (deuterated) solvent. After leaving the sample for 72 hours at room temperature, the ^{1}H NMR spectrum of the soluble fraction was recorded.

1.7 Recycling and self-healing test

The pristine material for the recycling test was prepared by hot-pressing (100 °C, 1 MPa, 15 min) the raw **P-XDA** materials into bars with a dimension of 1.5 × 1.0 × 0.1 cm (length × width × thickness). Afterwards, the samples were left for 1 day at ambient atmosphere before being measured. DMA was then used to stretch the materials at a constant stretching speed of 10% per min until the sample reached its maximal elongation and either snapped or flowed. Four samples were measured and the average values for yield point (%), yield stress (MPa), elongation at break (%) and Young's modulus (MPa) were reported. For the following recycling steps, the materials were cut into small pieces (approximately 0.2 cm^2) and again hot-pressed in a similar fashion as before (Fig. S6). The recycled samples were again measured in sets of four as described. A total of 4 cycles was performed (1 of the pristine material and 3 recycling steps).

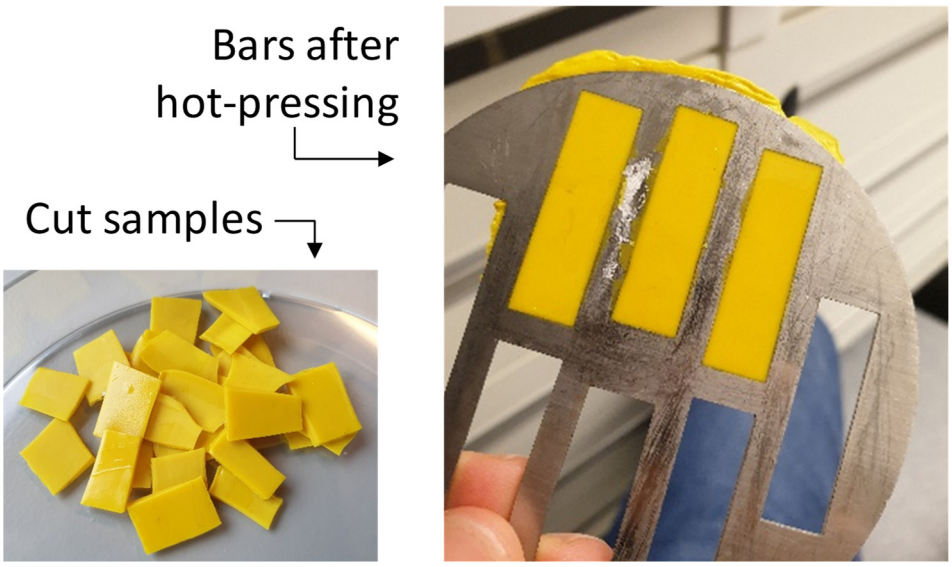

*Fig. S6 Photos of the cut **P-TDA** material and of the bars (still in the mould) after hot-pressing.*

For the self-healing experiment bars of the same dimension were prepared, which were then cut in half. The two halves were placed back into the mould so that the cut edges would touch each other. The experiment was carried out at 25, 50 and 75 °C without applying external pressure. Full self-healing of the material was achieved within 2 hours at 50 and 75 °C, and 25 hours at 25 °C. The healed samples (Fig. S7) were then tested for their material properties using the same DMA procedure as the recycling experiment.

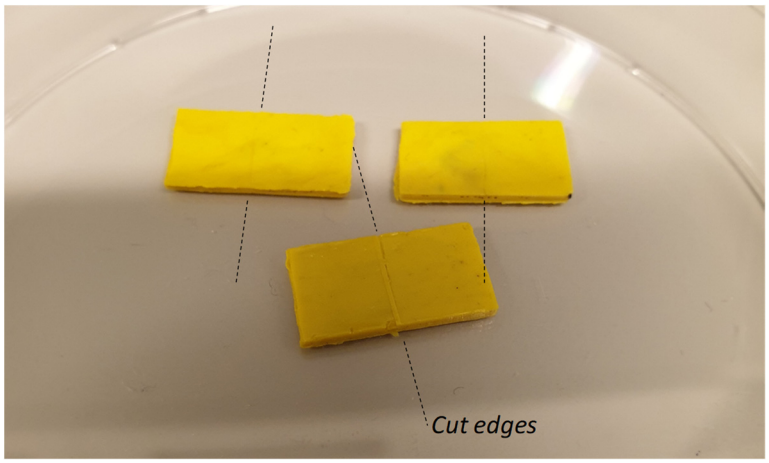

*Fig. S7 Photo of healed **P-TDA** samples. Dotted lines represent the edges where the material was cut in half.*

2. Hammett values (σ)

Chart S1 gives an overview of the five tuneable dianilines (**XDAs**) used in this study, and their corresponding Hammett parameter (σ). The σ values were chosen from their most structurally similar compound used in Hammett studies,[S3, S4] which are shown as well. For all cases the σ value for the para-substituent (σ_p) was used.

*Chart S1 Overview of **XDA** monomers, their corresponding Hammett value (σ) values, and the structures of which the σ values were derived from.*[S3, S4]

XDA monomer	Monomer structure	σ_p	Derived from:
ODA	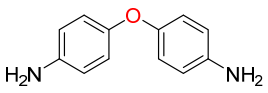	-0.03	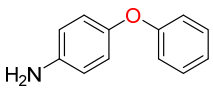
TDA	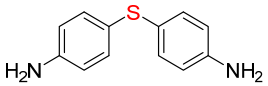	0.07	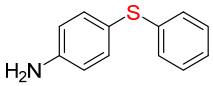
KDA	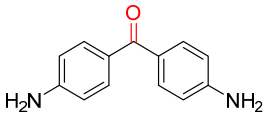	0.43	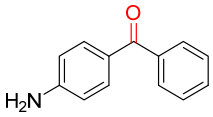
FDA	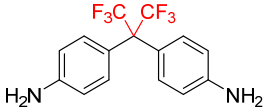	0.55	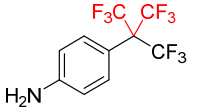
SDA	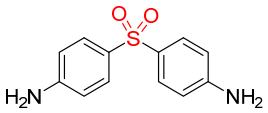	0.68	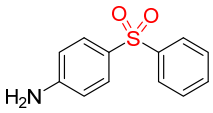

3. IR spectra of P-XDA materials

Fig. S8A shows the IR spectrum of terephthalaldehyde, as the aldehyde starting material for the **P-XDA** polymers. The aldehyde signal at 1700 cm^{-1} is indicated by an orange line. The IR spectra of the **P-XDA** materials (Fig. S8B–F) show disappearance of the (conjugated) aldehyde signal at 1700 cm^{-1} (highlighted in orange) and appearance of the imine signal at 1640 cm^{-1} (highlighted in blue), and thus provide evidence for the conversion of aldehyde into imine.

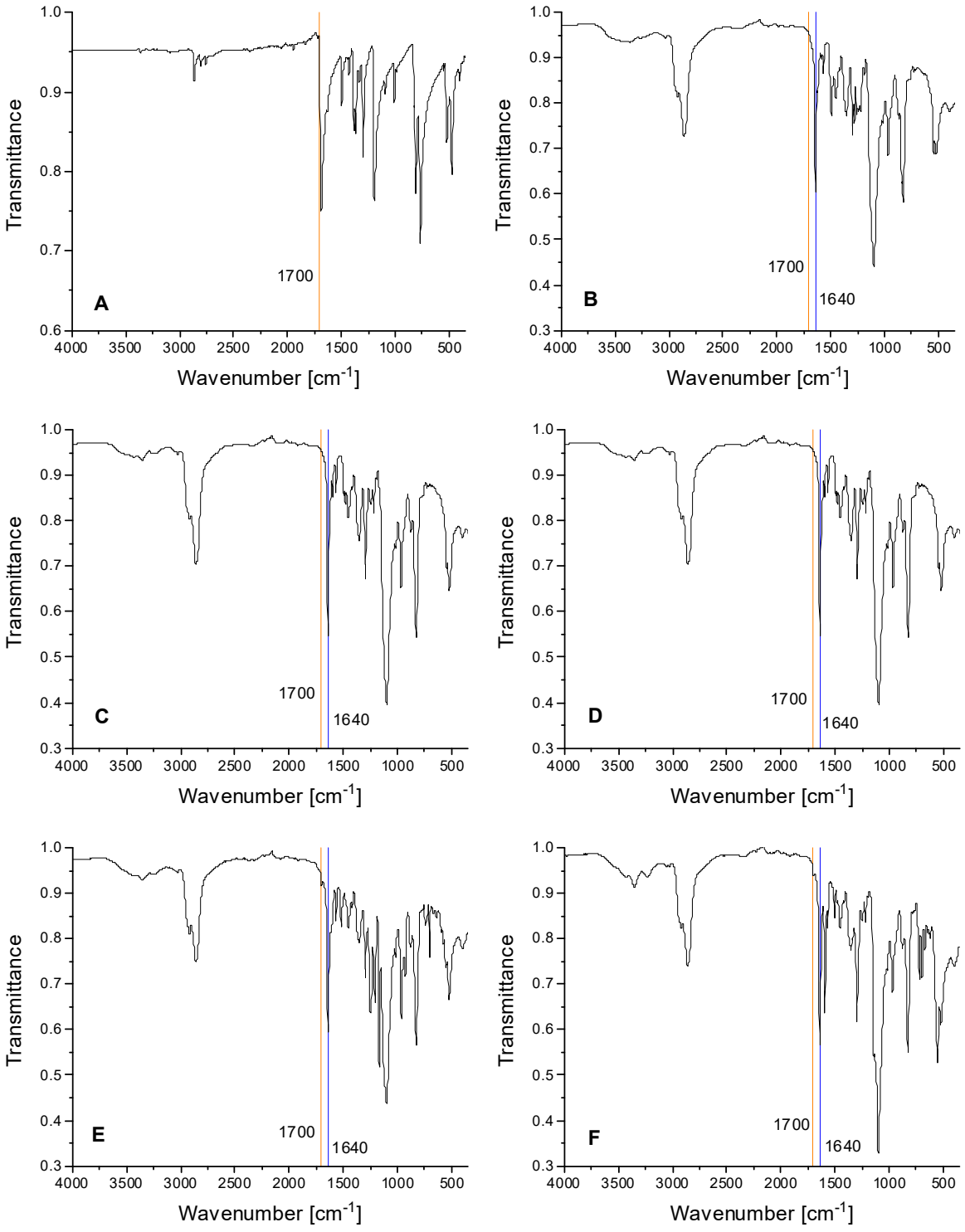

Fig. S8 IR spectrum of A) terephthalaldehyde, B) ***P-ODA****, C)* ***P-TDA****, D)* ***P-KDA****, E)* ***P-FDA****, F)* ***P-SDA*** *. The aldehyde signals (1700 cm^{-1}) are highlighted in orange and the imine signals (1640 cm^{-1}) are highlighted in blue. Note that the residual aldehyde signal in E and F account for less than 5% (based on integration), compared to the corresponding imine signal.*

4. Determination of ideal monomer ratios

To determine the ideal contents of dianiline and **TOTDDA** in the polymer system, three samples with different dianiline contents (Table S2) were prepared following the standardised synthetic procedure. As this was an indicative experiment, only **TDA** was used in this test. The crosslinker (**TREN**) content was first tested at 5 mol%, and was concluded to be a satisfactory amount. Using rheology, a temperature sweep experiment was performed on a temperature range of 20–150 °C for each of the three materials. A constant strain of 0.1% and angular frequency of 1 Hz was applied. The tan(δ) was plotted as a function of the temperature to obtain the curves presented in Fig. S9. As seen in the figure, a dianiline content of 30% resulted in the material to be relatively unsusceptible for changes in temperature below 150 °C. On the other hand, a dianiline content of 10% resulted in the material to initiate fast liquification already before 100 °C, as tan(δ) = 1 was observed at 75 °C and increased rapidly thereafter. The material incorporating 20% of dianiline showed ideal behaviour as the material displayed a distinct temperature dependency, but also the effect was delicate enough in order for the dianiline to serve as a tuneable handle.

*Table S2 List of tested dianiline ratios in **P-TDA** materials. Note that **TREN** has 3 amine groups, whereas **TDA** and **TOTDDA** have 2 amine groups. Therefore the 5% of **TREN** nets to 7.5% of amine relative to the aldehyde content, adding the total to 100%. To form the polymer network an equimolar amount (100%) of terephthalaldehyde was added to provide full conversion of amines to imines.*

Entry	TDA [%]	TOTDDA [%]	TREN [%]
1	10	87.5	5.0
2	20	77.5	5.0
3	30	65.5	5.0

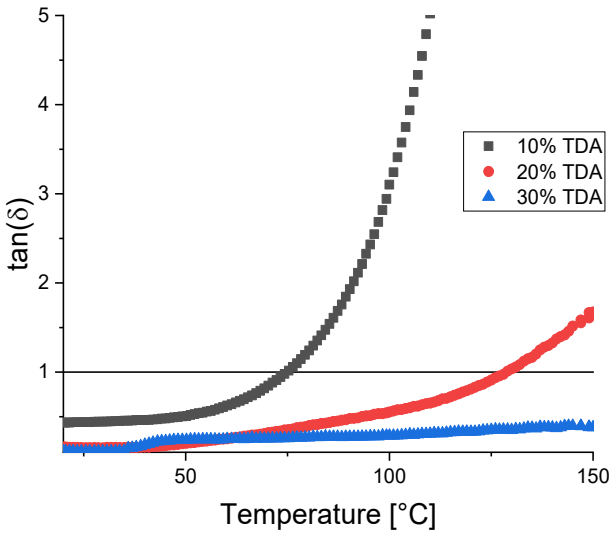

*Fig. S9 Tan(δ) curves for polyimine materials with 10% (black squares), 20% (red spheres) and 30% (blue triangles) of **TDA** dianiline content. Tan(δ) = 1 for 10% dianiline at 75 °C, and increasing rapidly after. Tan(δ) = 1 for 20% dianiline at 129 °C. Tan(δ) for 30% dianiline remains below 1 for the entire duration of the experiment (up to 150 °C).*

5. Stress relaxation curves and Arrhenius plots

The stress relaxation curves and Arrhenius plots for all **P-XDA** materials from 10–50 °C are presented in Fig. S10–S19. The kinetic activation energies (E_a) as calculated from the Arrhenius plots are presented in Table S3. Note that the stress relaxation curves of **P-ODA** and **P-TDA**, suggest that (at least) two time scales for relaxation are present, which offers the potential to further study (and dissect) the relaxation behaviour of this type of dynamic systems. However, the main –short time scale– relaxation was found to follow Maxwell behaviour, while the temperature dependence of the relaxation time revealed Arrhenius behaviour. The data could therefore be analysed with the Maxwell model for stress relaxation ($G/G_0 = \exp[-t/\tau]$), followed by construction of an Arrhenius plot, which enabled construction of a meaningful Hammett plot (in which we observed a linear relation between activation energy and Hammett value; see Fig. 2C).

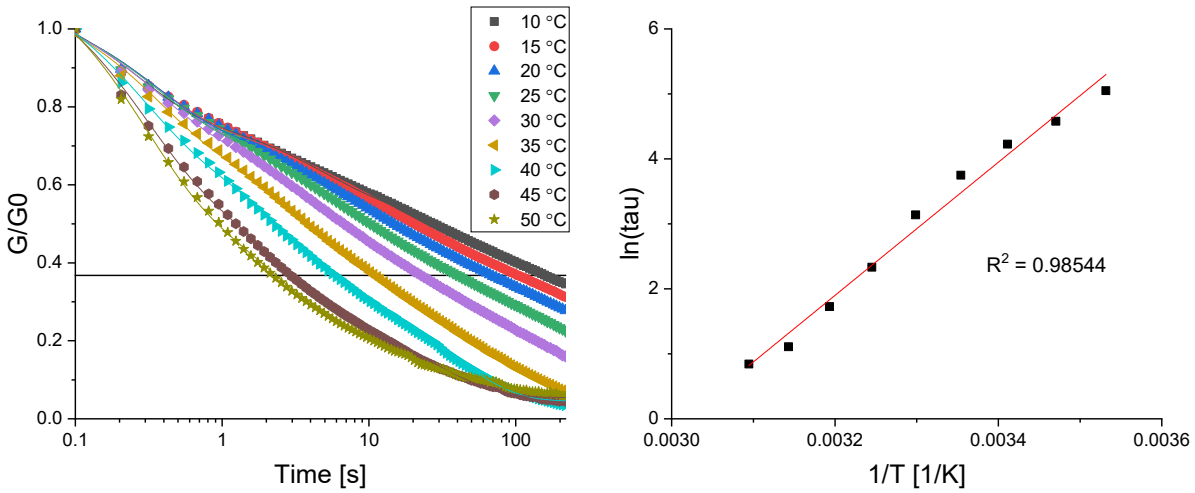

*Fig. S10 Stress relaxation curves (left) and Arrhenius plot (right) of **P-ODA**.*

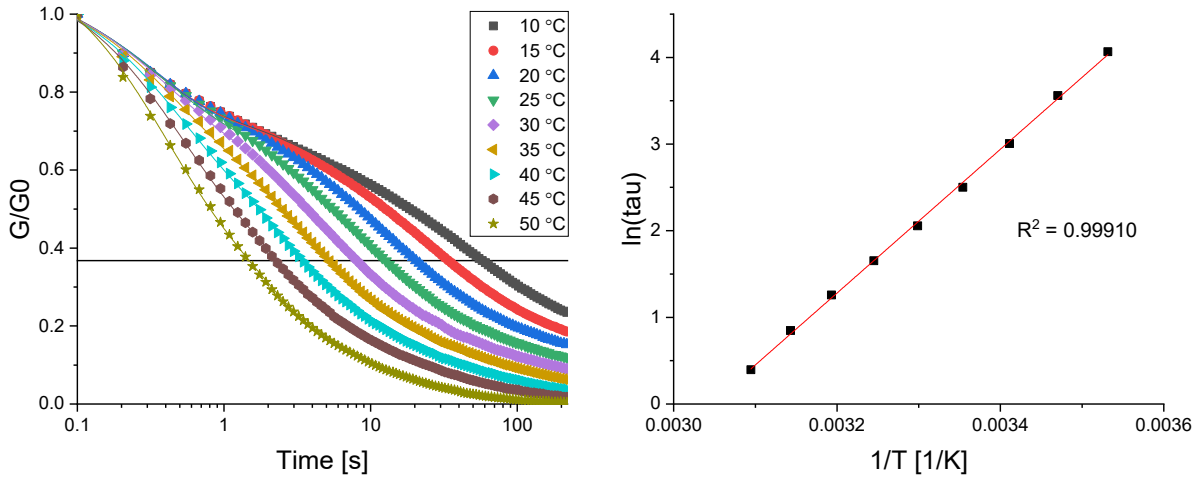

*Fig. S11 Stress relaxation curves (left) and Arrhenius plot (right) of **P-TDA**.*

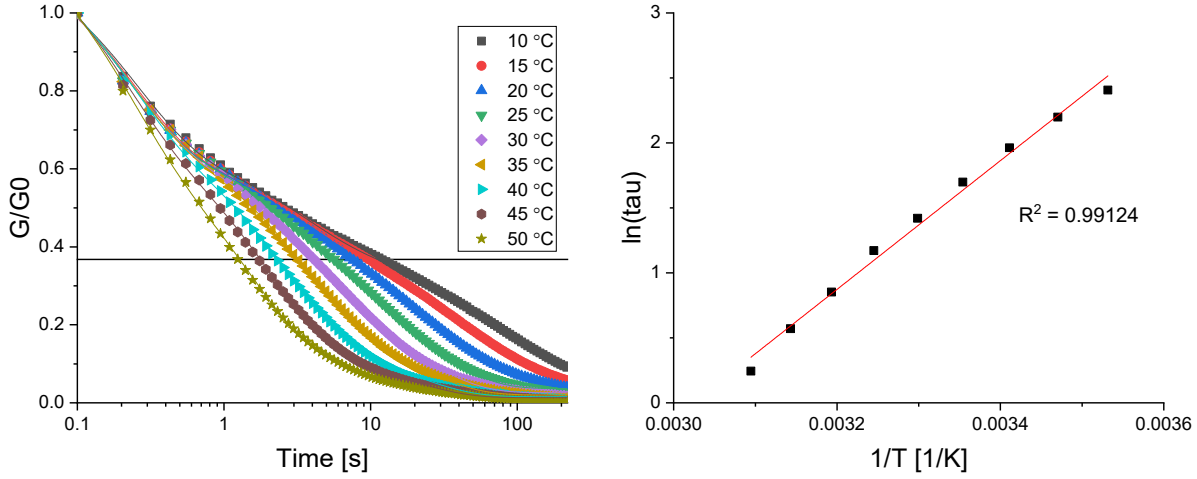

*Fig. S12 Stress relaxation curves (left) and Arrhenius plot (right) of **P-KDA**.*

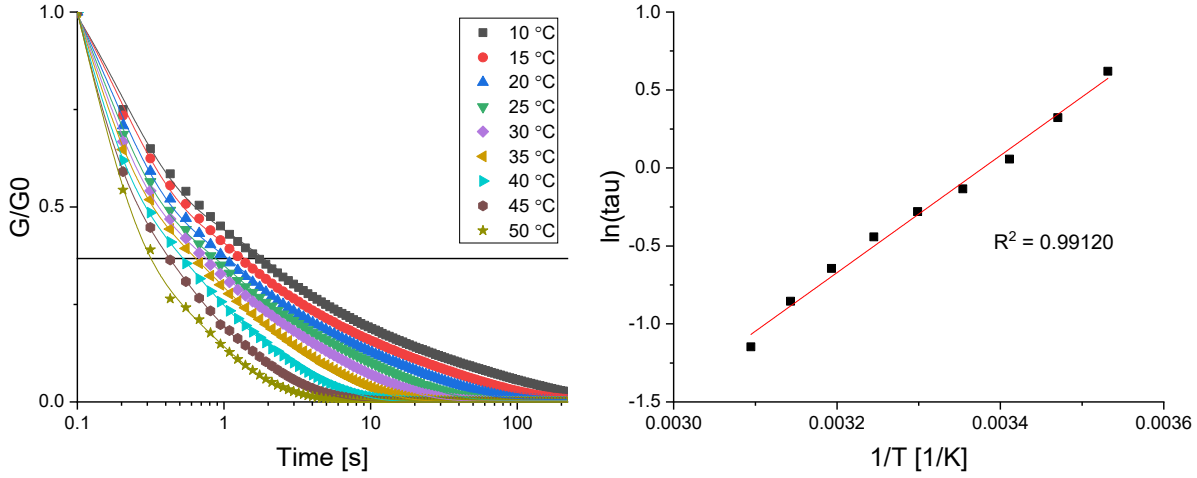

*Fig. S13 Stress relaxation curves (left) and Arrhenius plot (right) of **P-FDA**.*

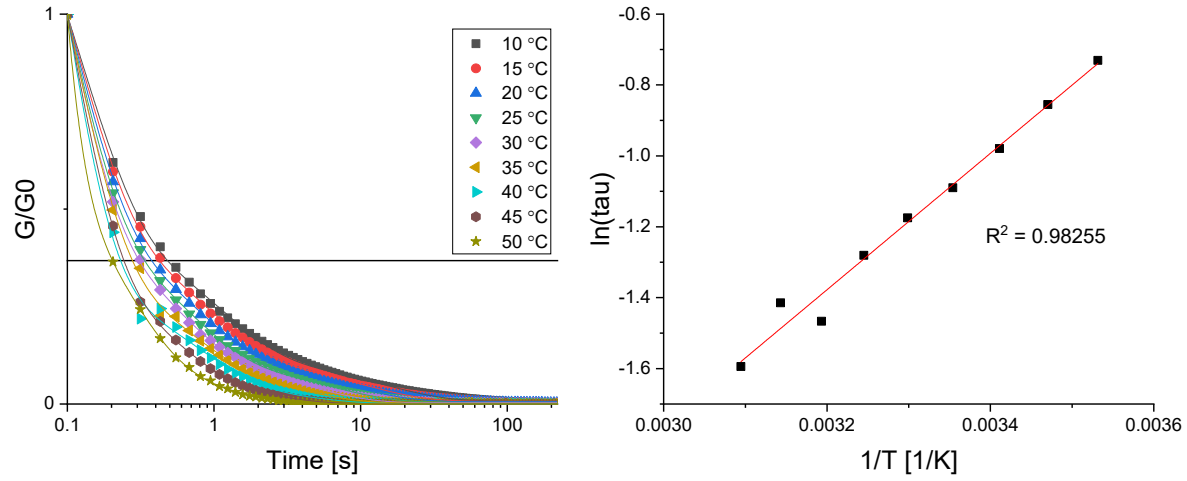

*Fig. S14 Stress relaxation curves (left) and Arrhenius plot (right) of **P-SDA**.*

*Table S3 Overview of calculated E_a values for all **P-XDA** materials.*

Material	E_a [kJ·mol^{-1}]
P-ODA	85 ± 4
P-TDA	69 ± 2
P-KDA	41 ± 1
P-FDA	31 ± 1
P-SDA	16 ± 1

6. Creep curves

Fig. S15A presents the combined curves of the creep experiment for all **P-XDA** materials. The data of the fitted curves as $\gamma = D * t^b$ are presented in Table S4. In Fig. S15B the strain at 1 s, 10 s, and 100 s, as a function of σ is visualised.

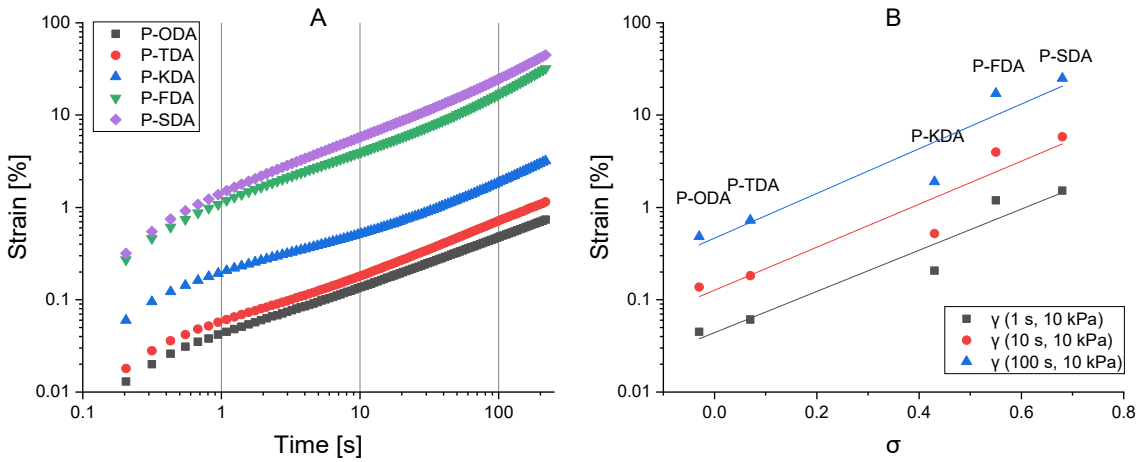

*Fig. S15 A) Combined curves for the strain over time for all **P-XDA** materials as a result of a constant stress of 10 kPa, and B) the strain at 1, 10 and 100 s as a function of the Hammett parameter (σ).*

Table S4 Overview of fitted parameters of the creep curves for where $\gamma = D * t^b$.

Material	*D*	*b*
P-ODA	0.0403 ± 0.0003	0.535 ± 0.002
P-TDA	0.0525 ± 0.0005	0.561 ± 0.003
P-KDA	0.172 ± 0.003	0.509 ± 0.005
P-FDA	1.06 ± 0.02	0.608 ± 0.005
P-SDA	1.33 ± 0.02	0.635 ± 0.004

7. Thermographic analysis

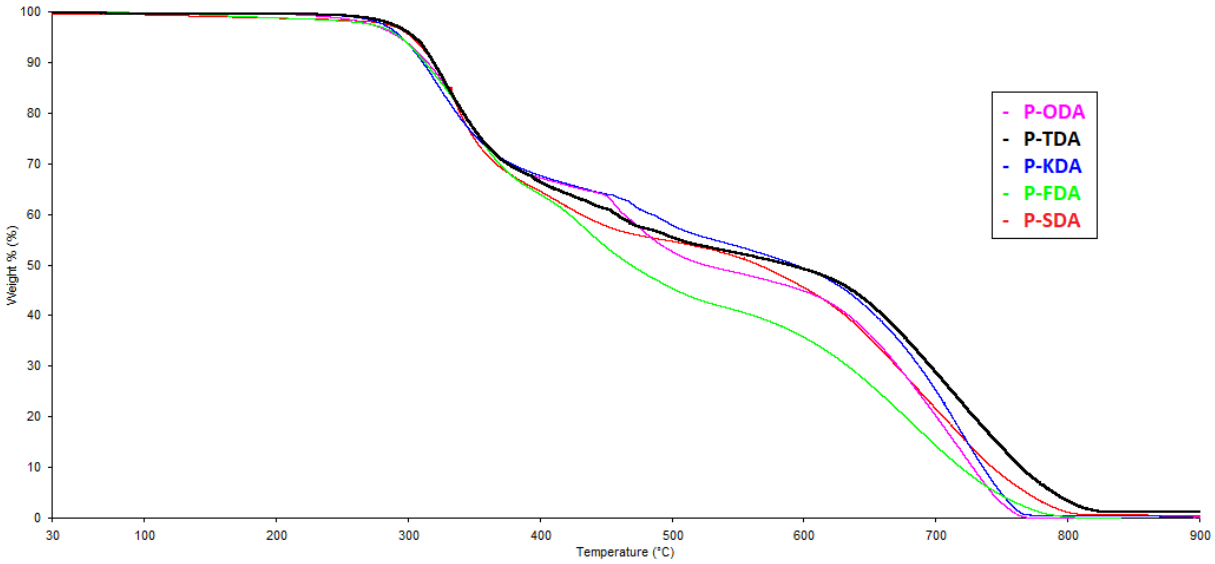

*Fig. S16 TGA curves for all five studied **P-XDA** materials. Degradation is measured as the remaining weight%, and plotted as a function of the temperature.*

All materials showed a degradation in three main steps (Fig. S16, Table S5). The first degradation step, for which 5 weight% of the initial material was lost ($T_{g5\%}$), was observed for all materials at 298 ± 6 °C. The second degradation step was observed at 406 ± 5 °C for the two most electron-withdrawing materials (**P-SDA** and **P-FDA**), and at 456 ± 9 °C for the three most electron-donating materials (**P-ODA**, **P-TDA** and **P-KDA**). The third degradation step was observed at 610 ± 6 °C for all materials. At 784 ± 23 °C all of the materials were fully degraded (>99% weight loss). From the heat flow curve of the TGA measurement T_g values were estimated, although with a relatively high uncertainty margin of ±5 °C. Note that T_g values determined by TGA generally differ from those obtained by rheology or DMA experiments. For the most electron withdrawing material, **P-SDA**, no T_g value was observed.

*Table S5 Overview of the degradation steps of the **P-XDA** materials obtained from the TGA measurements. Note: all temperature values are in °C. The T_g value for **P-SDA** could not be observed within the range of the measurement.*

Material	T_g	1st deg. step ($Tg_{5\%}$)	2nd deg. step	3rd deg. step	Full deg. pt. (>99% loss)
P-ODA	150	293	450	610	760
P-TDA	140	305	452	613	812
P-KDA	140	295	466	611	765
P-FDA	130	294	409	600	781
P-SDA	-	303	402	614	803

8. Temperature sweep curves

Temperature sweeps were performed for all materials from 0–150 °C. The materials were measured as discs with a 0.4 mm thickness and a 10 mm diameter. A constant strain of 0.1% and angular frequency of 1 Hz were applied. Storage (*G'*) and loss (*G''*) modulus were measured as a function of the temperature. Tan(*δ*) was calculated as *G''*/*G'*, and was plotted as a function of the temperature. All materials were measured *in triplo*, and representative tan(*δ*) curves are given for all materials in Fig. S17.

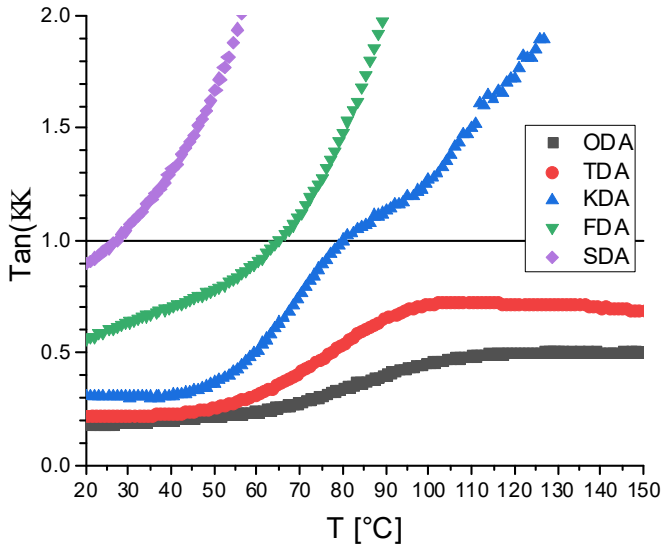

*Fig. S17 Combined plot of the tan(δ) as a function of the temperature for all **P-XDA** materials.*

9. Frequency sweep curves

Frequency sweeps for the **P-XDA** materials were performed on a frequency range of 0.1–100 Hz (Fig. S18A–E). The materials were measured as discs with a 0.4 mm thickness and a 10 mm diameter. All graphs were scaled to the same range for moduli (10^1–10^7 Pa). Red lines represent *G′* and blue lines represent *G″*. The darker colour represents a higher temperature. Every material was measured at 25, 50, 75 and 100 °C with a constant strain of 0.1%. As a general trend it could be observed that at lower frequencies both *G′* and *G″* rapidly drop, whereas at higher frequencies the moduli seemed to approach a plateau value (G_0). The presence of this plateau at near-similar values of *G′* for various temperatures indicates an associative exchange mechanism as the crosslinking density remains constant at all time, which is typical for vitrimers.[S5] The drop observed when the frequency decreases can be interpreted as a result of the material being able to relax via bond exchange reactions: an intrinsic feature of the imine bonds inside the material. When the frequency of the deformation is low, the materials have more time to relax and thus the moduli drop. At higher temperatures the materials have a shorter relaxation time due to an increased occurrence of bond exchange reactions. This shorter relaxation time enables the material to respond faster to deformations with higher frequencies. Therefore, a shift to the right, towards higher frequencies, of the curve is observed at higher temperatures. As an exploratory example, a time-temperature superposition (TTS) of the **P-TDA** data (Fig. S18B) indicated that the curves showed around a factor 10 shift in frequency at a temperature interval of 25 °C. However, this TTS was not further investigated and left for future analysis.

The materials incorporating the most electron-donating substituents (**P-ODA**, **P-TDA**, and **P-KDA**) all showed similar values for G_0, where $G' \approx 1$ MPa and $G'' \approx 0.5$ MPa. However, for the materials incorporating the most electron-withdrawing substituents (**P-FDA** and **P-SDA**) the plateau was not reached within in ranges of the experiment due to the higher frequency of bond exchange reactions, as was also concluded earlier in the stress relaxation experiments. Likewise, the drop in moduli at lower frequencies showed to be

more significant as the electron-withdrawing effect of the substituents increased. These results suggest that materials incorporating electron-withdrawing substituents respond faster to deformations with low frequencies due to shorter relaxation times.

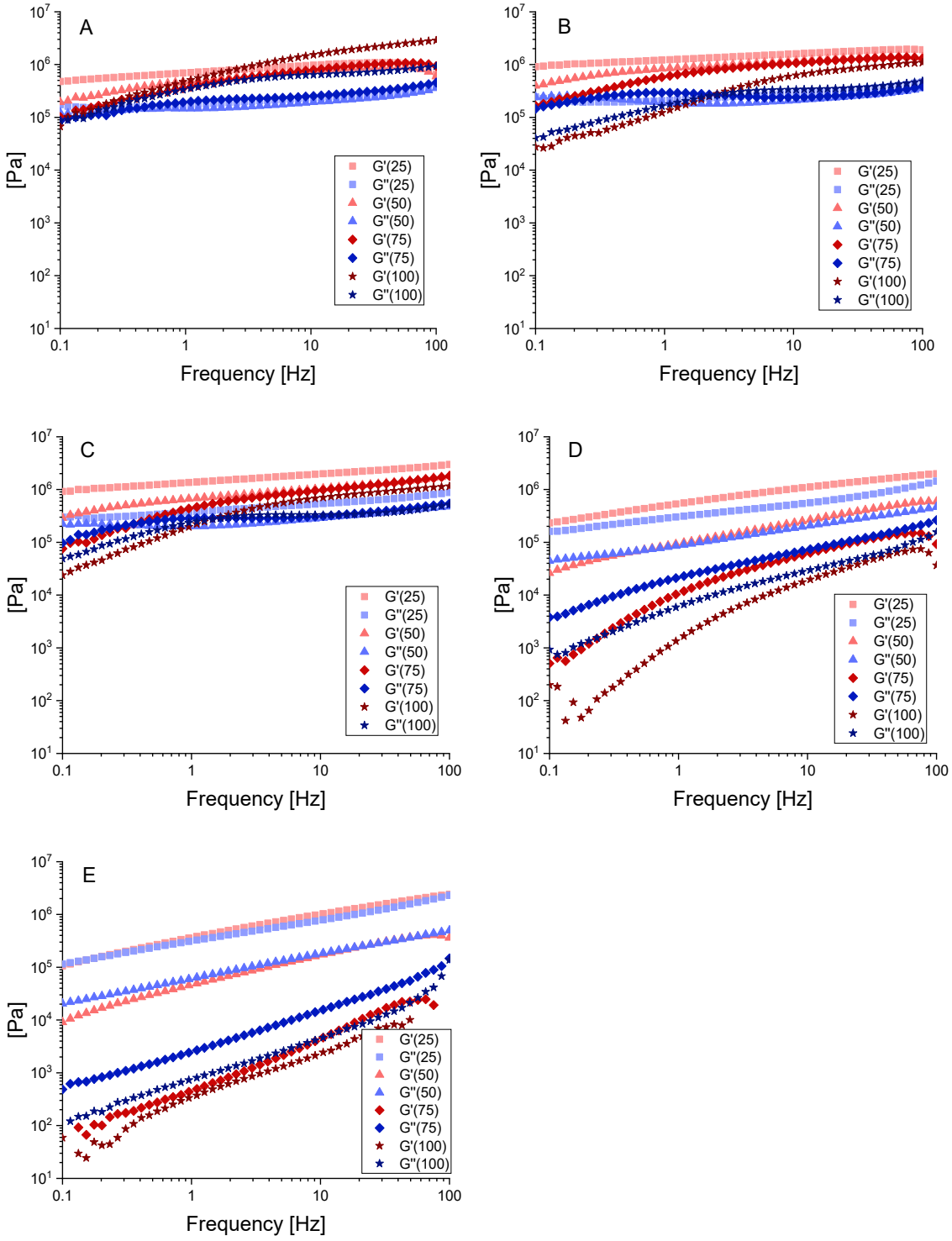

*Fig. S18 Frequency sweep curves at 25, 50, 75, and 100 °C for A) **P-ODA**, B) **P-TDA**, C) **P-KDA**, D) **P-FDA**, E) **P-SDA**. Red curved are of the storage modulus (G') and blue curves are of the loss modulus (G''). The darker grades of colours represent higher temperatures.*

10. Solubility studies

An overview of the non-dissolved fractions of **P-XDA** materials after the solubility experiment is presented in Table S6.

*Table S6 Overview of the non-dissolved fraction of **P-XDA** material after soaking the material in the corresponding solvent for 5 days at room temperature.*

Solvent	P-ODA	P-TDA	P-KDA
Heptane	0.98	0.99	0.98
Water	0.90	0.94	0.92
Acetonitrile	0.70	0.73	0.61
Methanol	0.44	0.41	0.32
THF	0.27	0.26	0.14
DCM	0.32	0.17	0.08

The dissolved fraction of **P-ODA** was further studied for three solvents: acetonitrile, dichloromethane and methanol by ^{1}H NMR spectroscopy, as is shown in Fig. S19 and S20.

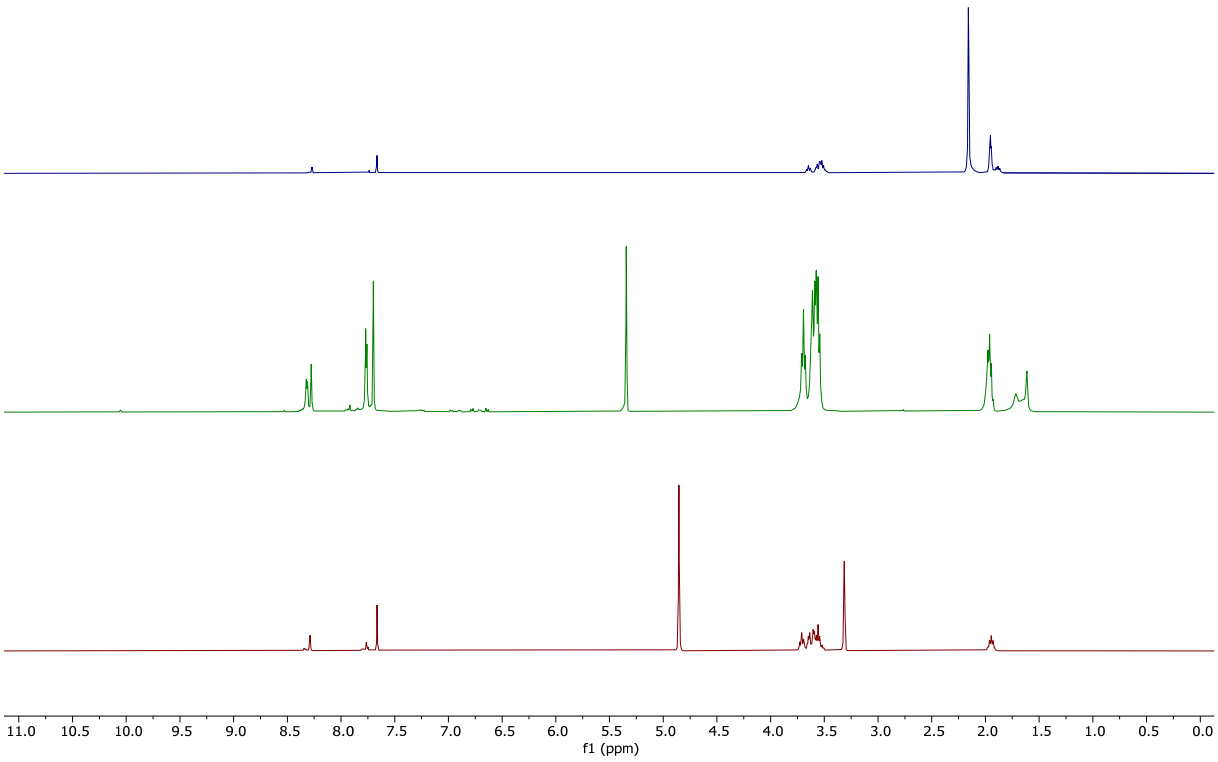

*Fig. S19. ^{1}H NMR spectrum of the dissolved fraction of **P-ODA** after immersion in CD_3CN (top), CD_2Cl_2 (middle) or CD_3OD (bottom) for 72 hours. See Fig. S20 for zoom in of the aldehyde/imine and aromatic region.*

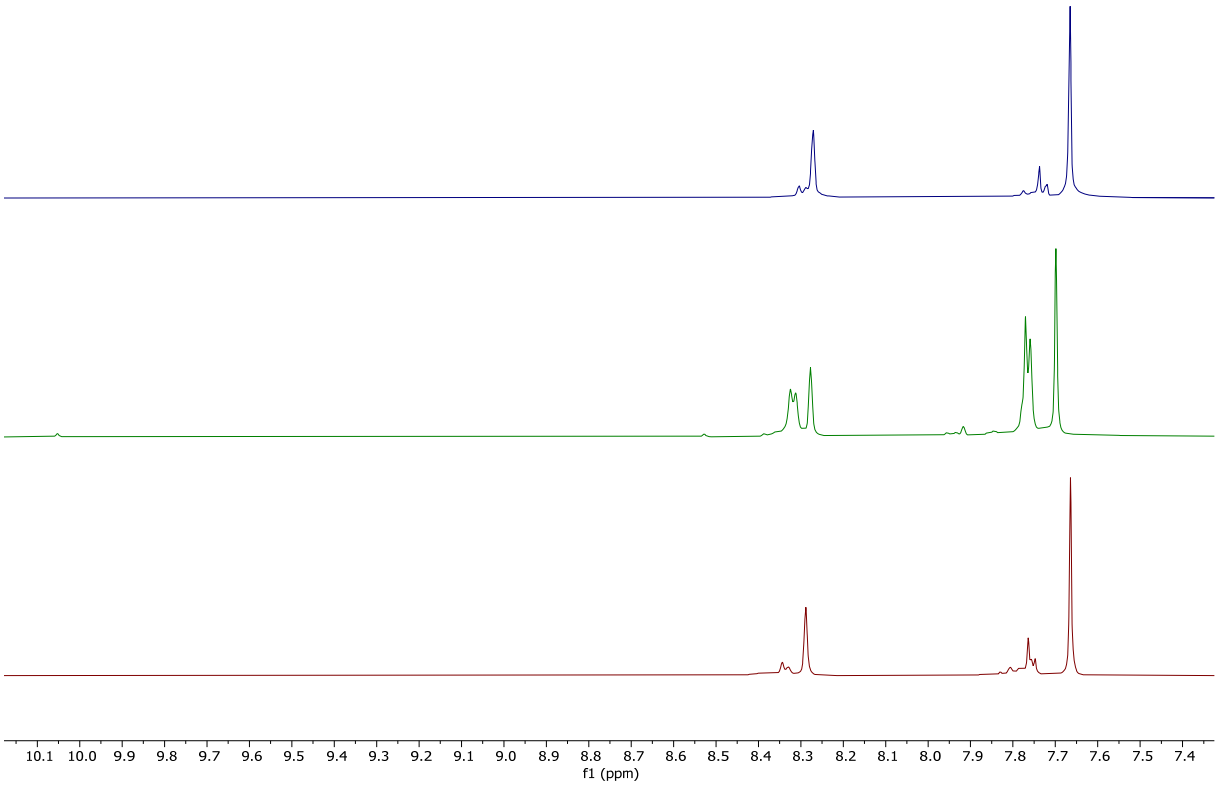

*Fig. S20. ^{1}H NMR spectrum –zoomed in on the aldehyde/imine and aromatic region– of the dissolved fraction of **P-ODA** after immersion in CD_3CN (top), CD_2Cl_2 (middle) or CD_3OD (bottom) for 72 hours. Note the absence of any aldehyde signal at 10.0 ppm in the case of CD_3CN and CD_3OD, while for CD_2Cl_2 only a very small aldehyde signal (which integrated to ~1% with respect to the imine signal at 8.3 ppm) can be discerned. See Fig. S19 for the full spectrum.*

11. Reprocessing and self-healing studies

Below, in Table S7 and S8 the results of the DMA studies of **P-TDA** and **P-ODA** after reprocessing and/or self-healing have been summarised.

*Table S7 Overview of DMA results for the reprocessing experiments of **P-TDA** (average of four measurements).*

Cycle	Yield point [%]	Yield stress [MPa]	Young's modulus [MPa]	Elongation at break [%]
1	19 ± 3	0.56 ± 0.03	11.3 ± 0.5	228 ± 24
2	20 ± 2	0.55 ± 0.04	11.2 ± 0.7	212 ± 24
3	20 ± 1	0.65 ± 0.01	11.7 ± 0.5	202 ± 11
4	21 ± 1	0.51 ± 0.01	10.3 ± 0.5	223 ± 28

*Table S8 Overview of DMA results for the reprocessing experiments of **P-ODA** (average of four measurements).*

Cycle	Yield point [%]	Yield stress [kPa]	Young's modulus [MPa]	Elongation at break [%]
1	45 ± 4	90 ± 6	0.51 ± 0.04	310 ± 33
2	39 ± 2	91 ± 6	0.49 ± 0.05	267 ± 17
3	46 ± 6	75 ± 4	0.47 ± 0.02	281 ± 37
4	46 ± 2	89 ± 8	0.49 ± 0.04	308 ± 19

*Table S9 Overview of DMA results for the self-healing experiments of **P-TDA** (average of four measurements).*

Conditions		Yield point [%]	Yield stress [kPa]	Young's modulus [MPa]
T [°C]	time [hr]			
Pristine		19 ± 3	0.56 ± 0.03	11.3 ± 0.5
25	24	19 ± 5	0.53 ± 0.02	11.3 ± 0.4
50	2	22 ± 4	0.58 ± 0.05	10.3 ± 0.7
75	2	22 ± 2	0.59 ± 0.02	10.2 ± 0.1

12. References

S1. P. Taynton, C. Zhu, S. Loob, R. Shoemaker, J. Pritchard, Y. Jin and W. Zhang, *Polym. Chem.*, 2016, **7**, 7052-7056.

S2. C. J. Kloxin and C. N. Bowman, *Chem. Soc. Rev.*, 2013, **42**, 7161-7173.

S3. C. Hansch, A. Leo, S. H. Unger, K. H. Kim, D. Nikaitani and E. J. Lien, *J. Med. Chem.*, 1973, **16**, 1207-1216.

S4. C. Hansch, A. Leo and R. W. Taft, *Chem. Rev.*, 1991, **91**, 165-195.

S5. A. Jourdain, R. Asbai, O. Anaya, M. M. Chehimi, E. Drockenmuller and D. Montarnal, *Macromolecules*, 2020, **53**, 1884-1900.